Rubisco Catalytic Properties and Temperature Response in Crops[1]

Carmen Hermida-Carrera, Maxim V. Kapralov, and Jeroni Galmés*

Research Group on Plant Biology under Mediterranean Conditions, Universitat de les Illes Balears, 07122 Palma, Balearic Islands, Spain (C.H.-C., J.G.); and School of Natural Sciences and Psychology, Liverpool John Moores University, Liverpool L3 3AF, United Kingdom (M.V.K.)

ORCID IDs: 0000-0003-3272-3054 (C.H.-C.); 0000-0001-7966-0295 (M.V.K.); 0000-0002-7299-9349 (J.G.).

Rubisco catalytic traits and their thermal dependence are two major factors limiting the CO_2 assimilation potential of plants. In this study, we present the profile of Rubisco kinetics for 20 crop species at three different temperatures. The results largely confirmed the existence of significant variation in the Rubisco kinetics among species. Although some of the species tended to present Rubisco with higher thermal sensitivity (e.g. *Oryza sativa*) than others (e.g. *Lactuca sativa*), interspecific differences depended on the kinetic parameter. Comparing the temperature response of the different kinetic parameters, the Rubisco K_m for CO_2 presented higher energy of activation than the maximum carboxylation rate and the CO_2 compensation point in the absence of mitochondrial respiration. The analysis of the Rubisco large subunit sequence revealed the existence of some sites under adaptive evolution in branches with specific kinetic traits. Because Rubisco kinetics and their temperature dependency were species specific, they largely affected the assimilation potential of Rubisco from the different crops, especially under those conditions (i.e. low CO_2 availability at the site of carboxylation and high temperature) inducing Rubisco-limited photosynthesis. As an example, at 25°C, Rubisco from *Hordeum vulgare* and *Glycine max* presented, respectively, the highest and lowest potential for CO_2 assimilation at both high and low chloroplastic CO_2 concentrations. In our opinion, this information is relevant to improve photosynthesis models and should be considered in future attempts to design more efficient Rubiscos.

The reported stagnation in the annual gains of cereal yields in the last decade clearly indicates that the expected demand for increased yield, at least 50% by 2050 (http://www.fao.org/economic/ess/ess-home/en/), will not be met by conventional breeding (Zhu et al., 2010). Future improvements will come from novel bioengineering approaches specifically focused on processes limiting crop productivity that have not been addressed so far (Parry and Hawkesford, 2012; Ort et al., 2015). A number of specific modifications to the primary processes of photosynthesis that could increase canopy carbon assimilation and production through step changes include the modification of the catalytic properties of Rubisco (Murchie et al., 2009; Whitney et al., 2011; Parry et al., 2013; Ort et al., 2015). First, biochemical models indicate that CO_2 fixation rates are limited by Rubisco activity under physiologically relevant conditions (Farquhar et al., 1980; von Caemmerer, 2000; Rogers, 2014). Second, Rubisco's catalytic mechanism exhibits important inefficiencies that compromise photosynthetic productivity: it is a slow catalyst, forcing plants to accumulate large amounts of the protein, and unable to distinguish between CO_2 and oxygen, starting a wasteful side reaction with oxygen that leads to the release of previously fixed CO_2, NH_2, and energy (Roy and Andrews, 2000). These inefficiencies limit not only the rate of CO_2 fixation but also the capacity of crops for an optimal use of resources, principally water and nitrogen (Flexas et al., 2010; Parry and Hawkesford, 2012).

Rubisco kinetic parameters has been described in vitro at 25°C for about 250 species of higher plants, of which only approximately 8% are crop species (Yeoh et al., 1981; Bird et al., 1982; Sage, 2002; Ishikawa et al., 2009; Prins et al., 2016). These data revealed the existence of significant variability in the main Rubisco kinetic parameters both among C_3 species (Yeoh et al., 1980, 1981; Bird et al., 1982; Jordan and Ogren, 1983; Parry et al., 1987; Castrillo, 1995; Delgado et al., 1995; Kent and Tomany, 1995; Balaguer et al., 1996; Bota et al., 2002; Galmés et al., 2005, 2014a, 2014c; Ghannoum et al., 2005; Ishikawa et al., 2009) and between C_3 and C_4 species (Kane et al., 1994; Sage, 2002; Kubien et al., 2008; Perdomo et al., 2015b). The existence of Rubiscos with different catalytic traits implies that the success,

[1] This study was supported by the Spanish Ministry of Science and Innovation (project nos. AGL2009–07999 and AGL2013–42364R to J.G.) and the Spanish Ministry of Education (FPI fellowship no. BES–2010–030796 to C.H.-C.).

* Address correspondence to jeroni.galmes@uib.cat.

The author responsible for distribution of materials integral to the findings presented in this article in accordance with the policy described in the Instructions for Authors (www.plantphysiol.org) is: Jeroni Galmés (jeroni.galmes@uib.cat).

J.G. conceived the project; C.H.-C. and J.G. designed the experiment; C.H.-C. performed the experiments; C.H.-C., M.V.K., and J.G. analyzed the data and wrote the article.

www.plantphysiol.org/cgi/doi/10.1104/pp.16.01846

in terms of photosynthetic improvement, of Rubisco engineering approaches in crops will depend on the specific performance of the native enzyme from each crop species. Nevertheless, our knowledge of the actual variability in Rubisco kinetics is still narrow, not only because of the limited number of species that have been examined so far but mainly because complete Rubisco kinetic characterization (including the main parameters) has been performed in very few species.

Recent modeling confirmed that Rubisco is not perfectly optimized to deliver maximum rates of photosynthesis and indicated that Rubisco optimization depends on the environmental conditions under which the enzyme operates (Galmés et al., 2014b). In particular, Rubisco catalytic parameters are highly sensitive to changes in temperature. For instance, the maximum carboxylase turnover rate (k_{cat}^{c}) increases exponentially with temperature (Sage, 2002; Galmés et al., 2015). However, at temperatures higher than the photosynthetic thermal optimum, the increases in k_{cat}^{c} are not translated into increased CO_2 assimilation because of the decreased affinity of Rubisco for CO_2 (i.e. higher Michaelis-Menten constant for CO_2 [K_c] and lower CO_2-oxygen specificity [$S_{c/o}$]) and the decreased CO_2-oxygen concentration ratio in solution (Hall and Keys, 1983; Jordan and Ogren, 1984). These changes favor the ribulose 1,5-bisphosphate (RuBP) oxygenation by Rubisco relative to carboxylation, increasing the flux through photorespiration and, ultimately, reducing the potential growth at high temperatures (Jordan and Ogren, 1984).

Beyond the discernment of the existing variability in Rubisco kinetics at a standard temperature, the knowledge of the temperature dependence of Rubisco kinetics and the existence of variability in the thermal sensitivity among higher plants are of key importance for modeling purposes. The number and diversity of plant species for which Rubisco kinetic parameters have been tested in vitro at a range of physiologically relevant temperatures are still very scarce (Laing et al., 1974; Badger and Collatz, 1977; Badger, 1980; Monson et al., 1982; Hall and Keys, 1983; Jordan and Ogren, 1984; Lehnherr et al., 1985; Uemura et al., 1997; Zhu et al., 1998; Sage et al., 2002; Galmés et al., 2005; Haslam et al., 2005; Yamori et al., 2006; Perdomo et al., 2015a; Prins et al., 2016) and mostly restricted to a few kinetic parameters; actually, there is no study examining the temperature dependencies of the main kinetic constants in the same species. The limited data reported so far suggest the existence of interspecific differences in the temperature dependence of some Rubisco kinetic parameters, like k_{cat}^{c} (Chabot et al., 1972; Weber et al., 1977; Sage, 2002) or $S_{c/o}$ (Zhu et al., 1998; Galmés et al., 2005). Actually, differences in the energy of activation of k_{cat}^{c} and $S_{c/o}$ seem to be ascribed to the thermal conditions typically encountered by the species in their native habitat (Galmés et al., 2005) as well as to the photosynthetic mechanism (Perdomo et al., 2015a).

The variability in the response of Rubisco kinetics to changes in temperature, if confirmed, is of paramount importance. The mechanistic models of photosynthesis at leaf, canopy, and ecosystem levels are based on the kinetic properties of Rubisco (Farquhar et al., 1980; von Caemmerer, 2000; Bernacchi et al., 2002), and the accuracy of these photosynthetic models depends on knowing the Rubisco kinetic parameters and the species-specific equations for the Rubisco-temperature dependencies (Niinemets et al., 2009; Yamori and von Caemmerer, 2009; Bermúdez et al., 2012; Díaz-Espejo, 2013; von Caemmerer, 2013; Walker et al., 2013). The need for estimations of the temperature dependencies of Rubisco kinetic parameters becomes timely as modelers try to predict the impact of increasing temperatures on global plant productivity (Sage et al., 2008; Gornall et al., 2010). Ideally, surveying variations in Rubisco kinetics and their temperature dependence should incorporate a correlative analysis with variations in the large (L)-subunit and/or small (S)-subunit amino acid sequence. Such a complementary research would permit deciphering what residue substitutions determine the observed variability in Rubisco catalysis.

In this study, we examined Rubisco catalytic properties and their temperature dependence in 20 crop species, thereby constituting the largest published data set of its kind. The aims of this work were (1) to compare the Rubisco kinetic parameters among the most economically important crops, (2) to search for differences in the temperature response of the main kinetic parameters among these species, (3) to test whether crop Rubiscos are optimally suited for the conditions encountered in plant chloroplasts, and (4) to unravel key amino acid replacements putatively responsible for differences in Rubisco kinetics in crops.

RESULTS

The Variability in Rubisco Kinetics at 25°C among the Most Relevant Crop Species

When considering exclusively the 18 C_3 crop species, at 25°C, the Rubisco Michaelis-Menten constant for CO_2 under nonoxygenic (K_c) and 21% O_2 (K_c^{air}) varied approximately 2-fold and 3-fold, respectively, and the k_{cat}^{c} varied approximately 2-fold (Table I). For K_c and K_c^{air}, *Manihot esculenta* presented the lowest values (K_c = 6.1 μM and K_c^{air} = 10.8 μM) and *Spinacia oleracea* presented the highest (K_c = 14.1 μM and K_c^{air} = 26.9 μM). Values for k_{cat}^{c} varied between 1.4 s^{-1} (*M. esculenta*) and 2.5 s^{-1} (*Ipomoea batatas*). The Rubisco $S_{c/o}$ was the kinetic parameter with the lowest variation among the C_3 species (Supplemental Fig. S1) and ranged between 92.4 mol mol^{-1} (*Solanum lycopersicum*) and 100.8 mol mol^{-1} (*Beta vulgaris* and *M. esculenta*; Table I). *Brassica oleracea* and *Glycine max* presented the lowest value for the Rubisco carboxylase catalytic efficiency, calculated as k_{cat}^{c}/K_c (0.17 s^{-1} μM^{-1}), and *Coffea arabica* presented the lowest value for the k_{cat}^{c}/K_c^{air} ratio (0.08 s^{-1} μM^{-1}). With regard to the oxygenase catalytic efficiency

Table I. *Kinetic parameters of crop Rubiscos measured at 25°C*

Parameters included K_c and K_c^{air}, k_{cat}^c, $S_{c/o}$, and the carboxylation (k_{cat}^c/K_c and k_{cat}^c/K_c^{air}) and the oxygenation (k_{cat}^o/K_o) catalytic efficiencies. The k_{cat}^o/K_o ratio was calculated as $(k_{cat}^c/K_c)/S_{c/o} \times 1{,}000$. For each species, data are means ± SE (n = 3–9). Group averages were obtained from individual measurements in each species. Different letters denote statistical differences ($P < 0.05$) by Duncan analysis between C_3 and C_4 groups.

Species	K_c	K_c^{air}	k_{cat}^c	$S_{c/o}$	k_{cat}^c/K_c	k_{cat}^c/K_c^{air}	k_{cat}^o/K_o
	μM	μM	s^{-1}	mol mol^{-1}	s^{-1} μM^{-1}	s^{-1} μM^{-1}	s^{-1} nM^{-1}
C_3 species							
Avena sativa	10.8 ± 0.9	18.1 ± 2.0	2.3 ± 0.3	99.9 ± 3.0	0.21 ± 0.01	0.13 ± 0.03	2.14 ± 0.06
Beta vulgaris	10.8 ± 1.2	18.6 ± 1.1	2.0 ± 0.3	100.8 ± 2.0	0.19 ± 0.02	0.10 ± 0.01	1.94 ± 0.31
Brassica oleracea	11.8 ± 0.1	19.2 ± 0.3	2.1 ± 0.3	96.2 ± 1.3	0.17 ± 0.03	0.11 ± 0.02	1.81 ± 0.28
Capsicum annuum	9.6 ± 0.3	19.8 ± 1.5	1.9 ± 0.1	96.0 ± 4.5	0.20 ± 0.01	0.10 ± 0.01	1.98 ± 0.15
Coffea arabica	11.0 ± 0.4	22.9 ± 2.4	2.1 ± 0.2	98.7 ± 3.8	0.19 ± 0.02	0.08 ± 0.01	1.98 ± 0.18
Cucurbita maxima	9.0 ± 0.5	19.2 ± 1.0	2.2 ± 0.2	98.4 ± 0.4	0.25 ± 0.04	0.12 ± 0.01	2.45 ± 0.31
Glycine max	8.6 ± 0.2	16.2 ± 0.7	1.5 ± 0.1	97.0 ± 1.1	0.17 ± 0.02	0.09 ± 0.01	1.76 ± 0.21
Hordeum vulgare	9.0 ± 0.6	14.9 ± 1.6	2.4 ± 0.2	99.2 ± 3.8	0.28 ± 0.02	0.17 ± 0.03	3.01 ± 0.19
Ipomoea batatas	12.0 ± 0.7	21.1 ± 1.0	2.5 ± 0.1	98.5 ± 6.6	0.20 ± 0.00	0.12 ± 0.01	1.96 ± 0.08
Lactuca sativa	11.1 ± 0.3	18.2 ± 1.4	2.2 ± 0.1	94.0 ± 1.9	0.19 ± 0.00	0.12 ± 0.01	2.06 ± 0.07
Manihot esculenta	6.1 ± 0.2	10.8 ± 0.6	1.4 ± 0.1	100.8 ± 0.9	0.23 ± 0.02	0.13 ± 0.01	2.24 ± 0.17
Medicago sativa	9.7 ± 1.6	16.4 ± 1.9	1.7 ± 0.1	95.6 ± 2.2	0.20 ± 0.02	0.11 ± 0.01	2.23 ± 0.36
Oryza sativa	8.0 ± 0.4	17.3 ± 2.4	2.1 ± 0.3	93.1 ± 1.2	0.26 ± 0.04	0.14 ± 0.03	2.73 ± 0.43
Phaseolus vulgaris	7.8 ± 0.3	14.0 ± 1.0	1.7 ± 0.2	99.7 ± 2.7	0.22 ± 0.02	0.13 ± 0.02	2.11 ± 0.17
Solanum lycopersicum	9.7 ± 0.4	16.6 ± 1.4	2.3 ± 0.2	92.4 ± 2.3	0.24 ± 0.02	0.14 ± 0.01	2.48 ± 0.20
Solanum tuberosum	9.6 ± 0.2	18.0 ± 0.8	2.0 ± 0.3	95.4 ± 2.3	0.22 ± 0.05	0.12 ± 0.03	2.32 ± 0.46
Spinacia oleracea	14.1 ± 0.8	26.9 ± 0.8	2.4 ± 0.1	97.0 ± 1.2	0.18 ± 0.01	0.09 ± 0.01	1.76 ± 0.13
Triticum aestivum	11.3 ± 0.4	16.0 ± 0.6	2.2 ± 0.2	100.1 ± 1.8	0.20 ± 0.02	0.14 ± 0.01	2.08 ± 0.24
C_3 average	10.0 ± 0.3a	18.0 ± 0.5a	2.1 ± 0.1a	97.5 ± 0.6a	0.21 ± 0.01a	0.12 ± 0.01a	2.17 ± 0.07a
C_4 species							
Saccharum × *officinarum*	26.3 ± 4.0	31.7 ± 2.1	3.9 ± 0.3	82.2 ± 1.8	0.15 ± 0.02	0.13 ± 0.01	1.82 ± 0.35
Zea mays	31.6 ± 1.8	42.0 ± 2.8	4.1 ± 0.6	87.3 ± 1.4	0.11 ± 0.02	0.07 ± 0.01	1.22 ± 0. 20
C_4 average	27.6 ± 2.3b	36.1 ± 2.6b	4.0 ± 0.5b	84.4 ± 1.5b	0.13 ± 0.02b	0.10 ± 0.01a	1.52 ± 0.23b

(calculated as k_{cat}^o/K_o), *S. oleracea* displayed the lowest value (1.76 s^{-1} nM^{-1}). *Hordeum vulgare* presented the highest values for the Rubisco carboxylase and oxygenase catalytic efficiencies (k_{cat}^c/K_c = 0.28 s^{-1} μM^{-1}, k_{cat}^c/K_c^{air} = 0.17 s^{-1} μM^{-1}, and k_{cat}^o/K_o = 3.01 s^{-1} nM^{-1}).

When data from the two C_4 species (*Saccharum* × *officinarum* and *Zea mays*) were included in the comparison at 25°C, the range of variability increased for all parameters (Table I). Rubisco from the two C_4 species presented higher k_{cat}^c but lower affinity for CO_2 (i.e. higher K_c and K_c^{air} and lower $S_{c/o}$) than Rubisco from C_3 crops. On average, k_{cat}^c/K_c and k_{cat}^o/K_o of C_4 Rubiscos were 62% and 70% of those of C_3 crop Rubiscos, respectively.

The Temperature Response of Rubisco Kinetics in Crops and Tradeoffs between Catalytic Traits

Both the range of variation and the species showing the extreme values of Rubisco kinetics at 15°C and 35°C were similar to those described at 25°C, with some exceptions. As at 25°C, among the C_3 crops, Rubisco from *M. esculenta* presented the lowest values for K_c and K_c^{air} at 15°C and 35°C, while the highest values were measured on Rubisco from *S. oleracea* (Supplemental Table S1). The lowest and highest values for k_{cat}^c at 15°C were those of Rubisco from *Cucurbita maxima* and *H. vulgare*, respectively. The degree of dispersion of the data and the range of variation between the maximum and minimum values for K_c, K_c^{air}, and k_{cat}^c increased with the increment in the assay temperature (Supplemental Table S1; Supplemental Fig. S1). Regarding $S_{c/o}$, values ranged between 116.1 mol mol^{-1} (*B. oleracea*) and 132.2 mol mol^{-1} (*C. maxima*) at 15°C and between 74.2 mol mol^{-1} (*Oryza sativa*) and 85 mol mol^{-1} (*M. esculenta*) at 35°C (Supplemental Table S1). As for $S_{c/o}$, the range of variation for k_{cat}^c/K_c and k_{cat}^o/K_o also was narrowed with the increase in the assay temperature (Supplemental Table S1; Supplemental Fig. S1).

Integrating all data across three assay temperatures, k_{cat}^c correlated positively with K_c for both C_3 species (r^2 = 0.82, $P < 0.001$) and C_4 species (r^2 = 0.94, $P < 0.001$), with Rubisco from C_4 species showing higher K_c for a given k_{cat}^c than that from C_3 species (Fig. 1A). The low interspecific variability in $S_{c/o}$ within each assay temperature determined a nonlinear relationship between k_{cat}^c and $S_{c/o}$ when considering data from all temperatures together (Fig. 1B). At each temperature individually, Pearson's correlation coefficients (PCCs) between k_{cat}^c and K_c and $S_{c/o}$ were highly significant (Table II) when considering both C_3 and C_4 together. The results from the PICs analyses were in general more conservative compared with PCCs (Table II), and some significant correlations were lost with PICs (e.g. $S_{c/o}$ versus K_c or K_c^{air} at 25°C). Notably, when excluding the two C_4 species, PCCs decreased in almost all

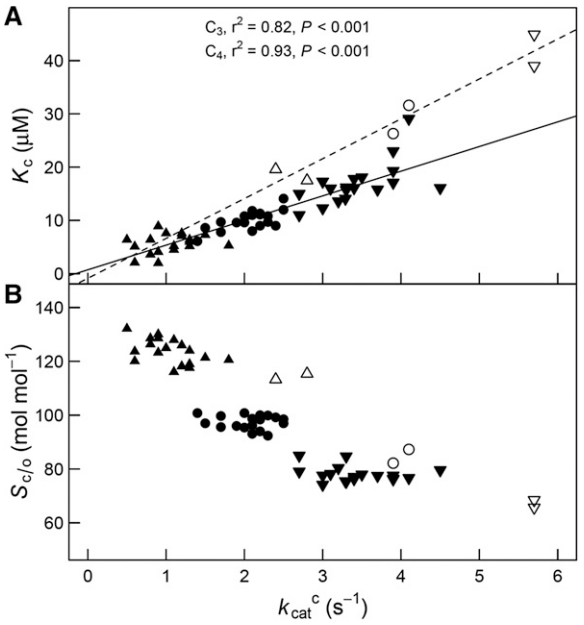

Figure 1. Relationship of k_{cat}^{c} with K_c (A) and the $S_{c/o}$ (B). Black symbols correspond to C_3 species at 15°C (triangles), 25°C (circles), and 35°C (inverted triangles); white symbols correspond to C_4 species at 15°C (triangles), 25°C (circles), and 35°C (inverted triangles). Each symbol represents the average value of a single species per temperature interaction.

correlations (Table II). Hence, the PCC between k_{cat}^{c} and K_c was no longer significant at 15°C, and the PCC between k_{cat}^{c} and $S_{c/o}$ was significant only at 15°C. Furthermore, when considering only C_3 species, the unique significant PICs between k_{cat}^{c} and K_c and $S_{c/o}$ were those found between k_{cat}^{c} and $S_{c/o}$ at 15°C and 25°C.

The energy of activation (ΔH_a) for K_c varied between 38.2 kJ mol^{-1} (*Solanum tuberosum*) and 83.1 kJ mol^{-1} (*O. sativa*; Table III). *I. batatas* (40.7 kJ mol^{-1}) and *M. esculenta* (75.4 kJ mol^{-1}) were the species showing the lowest and highest values for ΔH_a of K_c^{air}. As for k_{cat}^{c}, ΔH_a varied between 27.9 kJ mol^{-1} (*H. vulgare*) and 60.5 kJ mol^{-1} (*Medicago sativa*). Although the range of variation across C_3 species was similar for the energies of activation of both K_c and k_{cat}^{c} (2.2-fold), nonsignificant correlation was observed between ΔH_a for K_c and ΔH_a for k_{cat}^{c} in both conventional and phylogenetically independent analyses ($r^2 = 0.11$ and 0.15, respectively, $P > 0.05$). The lowest and highest values for ΔH_a of the CO_2 compensation point in the absence of mitochondrial respiration (Γ*; calculated from $S_{c/o}$) were measured in *B. vulgaris* (19.8 kJ mol^{-1}) and *G. max* (26.5 kJ mol^{-1}), respectively. On average, Rubisco from C_3 crops presented significantly higher ΔH_a for K_c (60.9 ± 1.5 kJ mol^{-1}) and k_{cat}^{c} (43.7 ± 1.5 kJ mol^{-1}) than Rubisco from C_4 species (K_c = 52.4 ± 5 kJ mol^{-1} and k_{cat}^{c} = 30.6 ± 1.6 kJ mol^{-1}). By contrast, nonsignificant differences were observed in the average ΔH_a for Γ* between C_3 species (22.9 ± 0.4 kJ mol^{-1}) and C_4 species (25 ± 0.7 kJ mol^{-1}).

The CO_2 Assimilation Potential of Rubisco Kinetics in Crops

The CO_2 assimilation potential of Rubisco ($A_{Rubisco}$) was modeled at varying temperature and CO_2 availability at the catalytic site (chloroplastic CO_2 concentration [C_c]) using the species-specific kinetic data measured at each temperature (Table I; Supplemental Table S1). The simulated value of C_c = 250 μbar is representative of that encountered in the chloroplast stroma of C_3 species under well-watered conditions (Bermúdez et al., 2012; Scafaro et al., 2012; Galmés et al., 2013). Under mild to moderate water stress, when no metabolic impairment is present, the decrease in the stomatal and leaf mesophyll conductances to CO_2 provokes a decrease in the concentration of CO_2 in the chloroplast (Flexas et al., 2006). We selected a value of 150 μbar to simulate the C_c in water-stressed plants.

Differences in $A_{Rubisco}$ across species were largely dependent on the temperature and the availability of CO_2 for carboxylation (Fig. 2). This fact was due to the different prevalence of RuBP-saturated (A_c) and RuBP-limited (A_j) CO_2 assimilation rates governing $A_{Rubisco}$ under the contrasting temperature and C_c, assuming an invariable concentration of active Rubisco sites of 25 μmol m^{-2} for all species. At 15°C, A_c limited $A_{Rubisco}$ at

Table II. *PICs (top part of the diagonals) and PCCs (bottom part of the diagonals) between the Rubisco kinetic parameters K_c, K_c^{air}, k_{cat}^{c}, and $S_{c/o}$ at 15°C, 25°C, and 35°C when considering the 20 C_3 and C_4 species together and the 18 C_3 species alone*

Significant correlations are marked with asterisks: ***, $P < 0.001$; **, $P < 0.01$; and *, $P < 0.05$.

	15°C				25°C				35°C			
	K_c	K_c^{air}	k_{cat}^{c}	$S_{c/o}$	K_c	K_c^{air}	k_{cat}^{c}	$S_{c/o}$	K_c	K_c^{air}	k_{cat}^{c}	$S_{c/o}$
Data from C_3 and C_4 species analyzed together												
K_c		0.826***	0.502*	−0.314		0.913***	0.819***	−0.202		0.960***	0.710***	−0.775***
K_c^{air}	0.927***		0.036	−0.099	0.946***		0.683***	0.037	0.962***		0.707***	−0.660**
k_{cat}^{c}	0.810***	0.645**		−0.660**	0.941***	0.890***		−0.450*	0.894***	0.858***		−0.634**
$S_{c/o}$	−0.498*	−0.361	−0.673**		−0.772***	−0.699***	−0.749***		−0.806***	−0.737***	−0.736***	
Data from C_3 species alone												
K_c		0.900***	0.194	0.120		0.646**	0.256	0.057		0.907***	0.363	−0.357
K_c^{air}	0.892***		−0.118	0.394	0.829***		0.173	−0.006	0.816***		0.401	−0.155
k_{cat}^{c}	0.268	0.137		−0.787**	0.698***	0.587*		−0.470*	0.613**	0.476*		−0.285
$S_{c/o}$	0.025	0.145	−0.496*		−0.049	−0.162	−0.083		−0.386	−0.157	−0.259	

Table III. *ΔH_a (kJ mol^{-1}) and c (dimensionless) values of K_c (μmol mol^{-1}) and K_c^{air} (μmol mol^{-1}), k_{cat}^c (s^{-1}), and Γ^* (μmol mol^{-1}) for the 20 crop species*

For each species, data are means ± SE (n = 3–9). Group averages were calculated from individual measurements in each species. Different letters denote statistical differences ($P < 0.05$) by Duncan analysis between C_3 and C_4 groups. Parameter concentrations of K_c (μM) and K_c^{air} (μM) in liquid phase (Table I; Supplemental Table S1) were converted to gaseous phase partial pressures (K_c and/or K_c^{air} [μmol mol^{-1}] = parameter [μM] × K_h × air volume [L]/RT]. K_h is the hydrolysis constant (15°C = 22.2, 25°C = 29.4, and 35°C = 38.2). For the air volume (L): 15°C = 23.7, 25°C = 24.5, and 35°C = 25.4. The term Γ^* (μmol mol^{-1}) is derived from $0.5O/S_{c/o}$, where O is the oxygen concentration.

Species	K_c		K_c^{air}		k_{cat}^c		Γ^*	
	c	ΔH_a	c	ΔH_a	c	ΔH_a	c	ΔH_a
C_3 species								
A. sativa	31.3 ± 0.7	63.4 ± 2.0	26.0 ± 0.4	48.9 ± 1.2	17.6 ± 2.2	41.5 ± 5.5	13.3 ± 0.5	23.6 ± 1.4
B. vulgaris	28.7 ± 1.7	57.0 ± 4.4	27.2 ± 0.7	51.8 ± 1.8	21.5 ± 3.7	51.2 ± 9.6	11.7 ± 0.4	19.8 ± 1.0
B. oleracea	28.1 ± 1.1	55.3 ± 2.8	26.5 ± 0.9	50.1 ± 2.4	18.8 ± 2.6	45.7 ± 6.5	12.6 ± 0.2	21.8 ± 0.5
C. annuum	26.6 ± 1.5	51.8 ± 3.7	27.0 ± 1.6	51.2 ± 3.7	16.3 ± 2.8	39.2 ± 6.9	13.4 ± 0.7	24.1 ± 1.8
C. arabica	34.7 ± 0.3	71.5 ± 0.9	27.6 ± 1.8	52.2 ± 4.3	16.5 ± 2.6	39.0 ± 6.1	13.1 ± 0.5	23.4 ± 1.1
C. maxima	28.6 ± 0.8	57.0 ± 1.8	29.2 ± 1.1	56.8 ± 2.8	20.2 ± 1.0	48.7 ± 2.7	12.2 ± 0.9	21.1 ± 2.2
G. max	34.2 ± 0.5	71.1 ± 1.4	28.4 ± 1.2	55.3 ± 2.9	22.7 ± 2.5	55.2 ± 5.8	14.4 ± 1.7	26.5 ± 4.1
H. vulgare	31.1 ± 1.1	63.4 ± 3.0	30.7 ± 1.9	60.9 ± 5.0	12.2 ± 1.6	27.9 ± 4.0	12.3 ± 0.2	21.2 ± 0.6
I. batatas	23.0 ± 0.7	42.4 ± 1.6	22.7 ± 1.2	40.7 ± 3.1	14.3 ± 1.5	33.4 ± 3.8	13.0 ± 0.3	22.8 ± 0.8
L. sativa	28.3 ± 1.3	55.8 ± 3.2	29.0 ± 2.1	56.5 ± 5.2	14.1 ± 0.7	33.3 ± 1.7	12.3 ± 0.3	21.2 ± 0.9
M. esculenta	33.7 ± 1.4	70.8 ± 3.4	36.1 ± 1.1	75.4 ± 2.8	19.8 ± 1.6	47.4 ± 4.1	12.2 ± 0.2	21.1 ± 0.5
M. sativa	29.2 ± 1.3	58.8 ± 3.6	26.1 ± 0.4	49.5 ± 1.0	24.8 ± 1.1	60.5 ± 2.8	11.8 ± 0.2	20.1 ± 0.4
O. sativa	38.9 ± 0.8	83.1 ± 1.8	30.5 ± 1.2	60.5 ± 3.1	19.2 ± 1.8	46.4 ± 4.7	13.7 ± 0.5	24.6 ± 1.3
P. vulgaris	31.5 ± 0.8	64.6 ± 2.0	30.9 ± 2.7	61.7 ± 6.8	19.8 ± 2.1	47.7 ± 5.3	13.4 ± 0.6	24.1 ± 1.5
S. lycopersicum	30.8 ± 2.5	62.1 ± 6.3	36.0 ± 2.5	73.8 ± 6.4	14.7 ± 1.4	34.6 ± 3.6	12.5 ± 0.2	21.8 ± 0.5
S. tuberosum	21.1 ± 0.2	38.2 ± 0.5	24.4 ± 0.8	44.9 ± 1.9	19.2 ± 0.5	46.2 ± 1.1	13.7 ± 0.9	24.7 ± 2.2
S. oleracea	34.3 ± 0.8	69.9 ± 2.2	25.1 ± 0.5	45.6 ± 1.1	20.2 ± 0.7	48.0 ± 1.8	13.5 ± 0.3	25.2 ± 1.0
T. aestivum	30.1 ± 0.5	60.4 ± 2.2	34.4 ± 2.2	70.1 ± 5.4	17.4 ± 1.7	41.2 ± 4.3	13.5 ± 0.2	24.2 ± 0.4
C_3 average	30.2 ± 0.6a	60.9 ± 1.5a	28.8 ± 0.6a	55.9 ± 1.5a	18.3 ± 0.6a	43.7 ± 1.5a	13.0 ± 0.2a	22.9 ± 0.4a
C_4 species								
S. officinarum	30.2 ± 1.9	58.3 ± 5.0	32.0 ± 1.0	62.3 ± 2.7	13.6 ± 1.5	30.2 ± 3.5	14.3 ± 0.6	25.8 ± 1.4
Z. mays	24.7 ± 3.4	44.5 ± 8.5	24.7 ± 3.4	44.5 ± 8.5	14.0 ± 0.9	31.0 ± 1.9	13.6 ± 0.1	24.3 ± 0.2
C_4 average	27.9 ± 2.0a	52.4 ± 5.0b	28.9 ± 0.8a	53.7 ± 1.9a	13.7 ± 0.7b	30.6 ± 1.6b	14.0 ± 0.3a	25. 0 ± 0.7a

C_c of 150 μbar in nine species (indicated by asterisks in Fig. 2). At 15°C and C_c of 250 μbar, only six species were A_c limited (*Capsicum annuum*, *C. maxima*, *M. sativa*, *O. sativa*, *S. tuberosum*, and *S. oleracea*). At 25°C and 35°C, $A_{Rubisco}$ was A_c limited in all C_3 species irrespective of C_c.

At 25°C, the best Rubisco was that from *H. vulgare* at both C_c values, while Rubisco from *G. max* yielded the lowest $A_{Rubisco}$ (Fig. 2). Rubisco from *B. vulgaris* presented the best performance at 35°C irrespective of CO_2 availability, while *C. annuum* and *S. officinarum* Rubisco gave the lowest $A_{Rubisco}$ at C_c of 250 and 150 μbar, respectively. At 15°C and C_c of 250 μbar, the highest potential for CO_2 assimilation was found in Rubisco from *G. max*, *M. esculenta*, and *Triticum aestivum*, while Rubisco from *M. esculenta* gave the highest $A_{Rubisco}$ at 15°C and C_c of 150 μbar. Rubisco from *C. maxima* displayed the lowest $A_{Rubisco}$ at 15°C, regardless of the CO_2 availability. It is interesting that Rubisco from the two C_4 species, in particular from *S. officinarum*, performed better than the average C_3 Rubiscos when $A_{Rubisco}$ was simulated according to the photosynthesis model for C_3 leaves (Farquhar et al., 1980), at 15°C and 25°C under C_c of 250 μbar (Fig. 2A). At lower C_c (150 μbar), the C_4 Rubiscos yielded higher $A_{Rubisco}$ values than the average C_3 Rubiscos at 15°C and lower values at 35°C, being similar at 25°C (Fig. 2B).

To test the performance of the different Rubiscos in the context of C_4 photosynthesis, A_c was also modeled assuming C_c of 5,000 μbar and concentration of active Rubisco sites (E) of 15 μmol m^{-2}. Under these conditions, the advantage of C_4-type Rubisco kinetics of *S. officinarum* and *Z. mays*, characterized by higher k_{cat}^c and K_c^{air}, became evident as providing higher A_c values at the three temperatures (data not shown). On average, at saturating CO_2 and lower concentration of Rubisco catalytic sites, C_4 Rubiscos yielded A_c of 35, 49, and 60 μmol m^{-2} s^{-1} at 15°C, 25°C, and 35°C, respectively, compared with the C_3 Rubisco averages (10, 23, and 42 μmol m^{-2} s^{-1}, respectively).

Positively Selected L-Subunit Residues: Relationship with Rubisco Kinetics

The phylogeny obtained with *rbcL*, *matK*, and *ndhF* genes matched the currently accepted angiosperm classification (Supplemental Fig. S2; Bremer et al., 2009). When considering all species together, 10 L-subunit residues were under positive selection: 94, 262, 281, 309, 439, 446, 449, 470, 477, and amino acid insert between residues 468 and 469. Moreover, positive selection was identified in specific L-subunit residues along branches leading to species with high and low K_c, high k_{cat}^c, and low

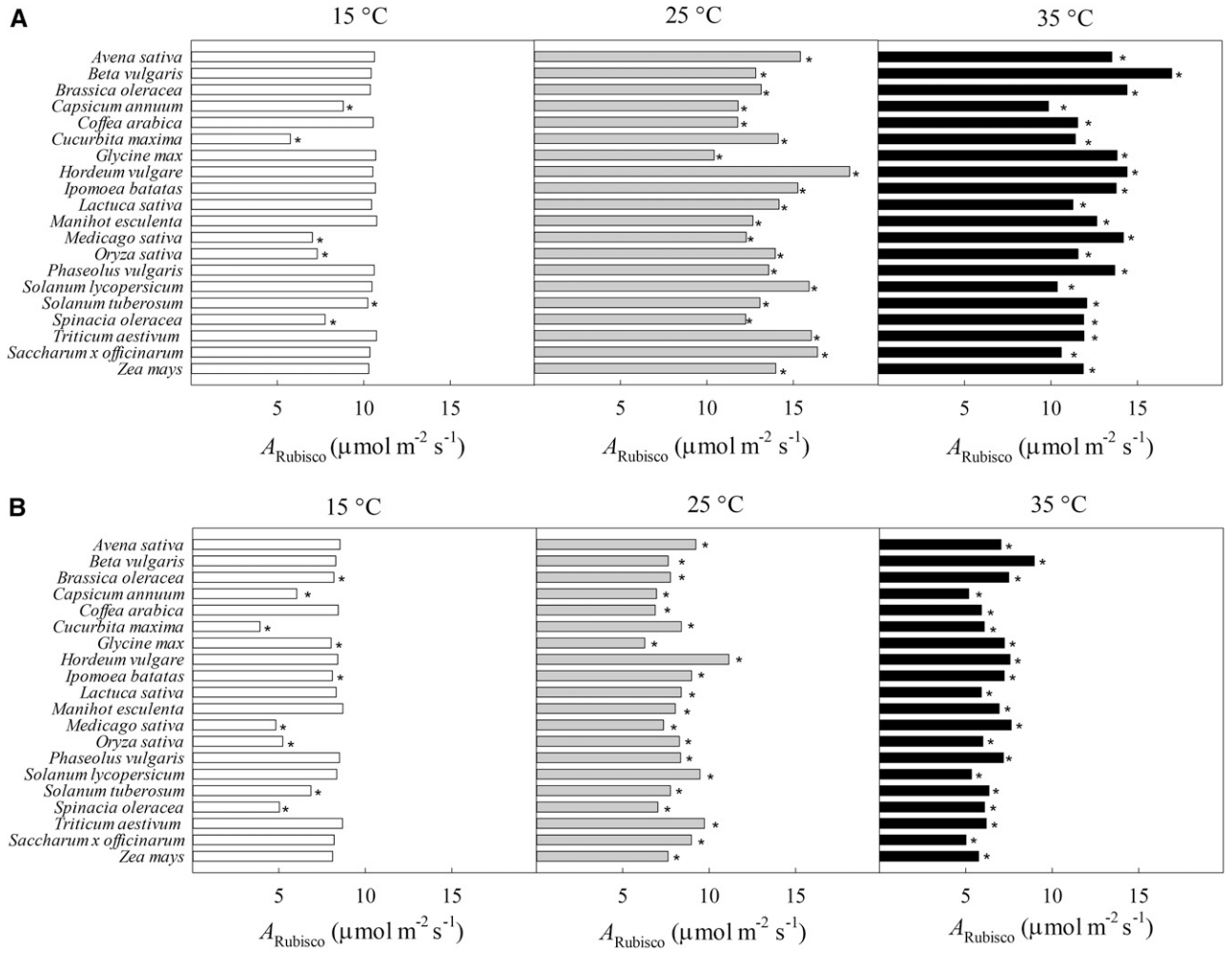

Figure 2. Simulated $A_{Rubisco}$ for C_3 and C_4 species at 15°C, 25°C, and 35°C and at C_c values of 250 μbar (A) and 150 μbar (B). Equations used to calculate $A_{Rubisco}$ were those described in the biochemical model of C_3 photosynthesis (Farquhar et al., 1980), as explained in "Materials and Methods." Bars represent minimum values of A_c- and A_j-limited $A_{Rubisco}$. Asterisks beside the bars indicate A_c-limited $A_{Rubisco}$, and the absence of asterisks indicates A_j-limited $A_{Rubisco}$. The rates of electron transport were 60, 150, and 212 μmol m^{-2} s^{-1} at 15°C, 25°C, and 35°C, respectively. The concentration of active Rubisco sites was assumed to be invariable at 25 μmol m^{-2} for all species and environmental conditions. The values used for the Rubisco kinetic parameters (k_{cat}^c, Γ*, and K_c^{air}) are those shown in Table I and Supplemental Table S1.

$S_{c/o}$ at 25°C and low ΔH_a for K_c (Table IV). The residues under positive selection were located at different positions within the Rubisco tertiary structure and included functionally diverse sites participating in L-subunit intradimer and dimer-dimer interactions and interactions with S-subunits and with Rubisco activase (Table IV). No residue under positive selection was associated with ΔH_a for K_c^{air}, ΔH_a for k_{cat}^c, or ΔH_a for $S_{c/o}$.

DISCUSSION

Main Crops Possess Rubiscos with Different Performance at 25°C

The kinetic data reported in this study are consistent with the range reported previously for higher plants at 25°C (Yeoh et al., 1980, 1981; Bird et al., 1982; Jordan and Ogren, 1983; Kent and Tomany, 1995; Galmés et al., 2005, 2014a, 2014c; Ishikawa et al., 2009; Prins et al., 2016; Table I) and showing the existence of significant variation among species in the carboxylase catalytic efficiency under nonoxygenic conditions (k_{cat}^c/K_c) and atmospheric conditions (k_{cat}^c/K_c^{air}). Recent reports related k_{cat}^c/K_c variation with the growth capacity in a group of closely related species with similar ecology (Galmés et al., 2014a), suggesting that improving this ratio would be an effective way to engineer a better Rubisco. Nevertheless, such an improvement becomes constrained by the tradeoffs between k_{cat}^c, K_c, and $S_{c/o}$ (Tcherkez et al., 2006; Savir et al., 2010; Galmés et al., 2014a, 2014c). Here, we demonstrate that these tradeoffs, in particular k_{cat}^c versus K_c, hold when considering

Table IV. *Amino acid replacements in the Rubisco L-subunit identified under positive selection by Bayes empirical Bayes analysis implemented in the PAML package (Yang et al., 2005; Yang, 2007) along branches of the phylogenetic tree leading to species with particular Rubisco properties*

Residue[a]	Amino Acid Changes	Location of Residue	Interaction[b]
Branches leading to species with $K_c \geq 26$ μM and $k_{cat}^c \geq 3.9$ s^{-1} at 25°C (C_4 species)			
94**	D, E, K → P		ID, RA
446**	R → K	C terminus	
469**	Insert of G or T before residue 469	C terminus	ID
Branches leading to species with $k_{cat}^c \geq 2.5$ s^{-1} at 25°C			
281**	A → S	Helix 4	DD, SS
Branches leading to species with $K_c \geq 10.8$ μM at 25°C			
439***	A → T, V	Helix G	
469*	Insert of G or T before residue 469	C terminus	ID
470*	A, E → K, P, Q	C terminus	ID
477**	S → E, G, P, Q	C terminus	
Branches leading to species with $S_{c/o} \leq 94$ mol mol^{-1} at 25°C			
309**	M → I	βF-strand	ID
Branches leading to species with ΔH_a for $K_c \leq 56$ kJ mol^{-1}			
262**	V → A, T	Loop 3	S-subunit
439*	R → T, V	Helix G	
449**	C, S, T → A	C terminus	
477**	K → E, G, P, Q	C terminus	

[a]Residue numbering is based on the *S. oleracea* sequence. Values for Bayesian posterior probabilities are as follows: *, >0.90; **, >0.95; and ***, >0.99. [b]Interactions in which the selected residues and/or residues within 5 Å of them are involved: DD, dimer-dimer interactions; ID, intradimer interactions; RA, interface for interactions with Rubisco activase; SS, interactions with small subunits (Ott et al., 2000; Spreitzer and Salvucci, 2002; Du et al., 2003).

C_3 and C_4 species together, even after accounting for the phylogenetic signal in the data, and that they generally strengthen at increasing assay temperatures (Table II). However, most of these tradeoffs were lost when considering exclusively the C_3 species (Table II), indicative that the broad-scale patterns of covariation between the Rubisco kinetic parameters may not hold at smaller scales, as observed previously in other angiosperm species (Galmés et al., 2014c).

The k_{cat}^c from *Z. mays* and *S. officinarum* was 2-fold higher than that of the C_3 species, albeit at the expense of 3 times less affinity for CO_2 (Table I). This finding agrees with previously described trends between C_3 and C_4 species (Ghannoum et al., 2005; Kubien et al., 2008; Ishikawa et al., 2009) and with the fact that C_4 species present lower k_{cat}^c/K_c (Kubien et al., 2008; Perdomo et al., 2015a).

Unlike other reports (Sage, 2002; Ishikawa et al., 2009), the observed variation in the kinetic parameters at 25°C among C_3 species was apparently not related to the thermal climate of their respective domestication regions (data not shown). It should be noted that the origin, and hence the climatic conditions, of the selected varieties could be different from the species center of domestication and that the different crop varieties may have accumulated adaptive changes to local conditions by means of artificial selection (Meyer et al., 2012). Intraspecific variability in Rubisco catalytic traits has been reported in *T. aestivum* (Galmés et al., 2014c) and *H. vulgare* (Rinehart et al., 1983), but how this variability among genotypes is related to the adaptation of Rubisco to local environments remains elusive.

The Rubisco Kinetic Parameters of the Main Crops Present Different Thermal Sensitivities

The observed temperature response of the Rubisco kinetic parameters confirms well-described trends of increases in k_{cat}^c and K_c and a decrease in $S_{c/o}$ with increasing assay temperature (Table I; Supplemental Table S1; Jordan and Ogren, 1984; Brooks and Farquhar, 1985; Uemura et al., 1997; Galmés et al., 2005; Prins et al., 2016).

The temperature dependency of full Rubisco catalytic constants was first provided for *Nicotiana tabacum* using in vivo-based leaf gas-exchange analysis (Bernacchi et al., 2001). After that report, all studies dealing with the temperature response of photosynthesis assumed the temperature dependency parameters of *N. tabacum* Rubisco, irrespective of the modeled species, from annual herbs to trees and from cold- to warm-adapted species (Pons et al., 2009; Keenan et al., 2010; Yamori et al., 2010; Galmés et al., 2011; Bermúdez et al., 2012; Scafaro et al., 2012). Importantly, our data set constitutes the most unequivocal confirmation that different temperature sensitivities of Rubisco kinetic parameters exist among different species and that extrapolating the temperature response of a unique model species to other plants induces errors when modeling the

temperature response of photosynthesis. In this sense, the in vitro results of this study support in vivo data showing different temperature dependencies of Rubisco catalytic constants in *Arabidopsis thaliana* and *N. tabacum* (Walker et al., 2013).

In general, the Rubisco constant affinities for CO_2 (K_c and K_c^{air}) were more sensitive to changes in the assay temperature (i.e. presented higher ΔH_a) than k_{cat}^c and Γ^* (Table III), in agreement with a recent study (Perdomo et al., 2015a). This fact is explained by the increase in the oxygenase catalytic efficiency (k_{cat}^o/K_o) at increasing temperature. However, it should be remarked that the k_{cat}^o/K_o ratio was calculated from the measured parameters K_c, k_{cat}^c, and $S_{c/o}$ and that direct measurements of the oxygenase activity of Rubisco (e.g. by mass spectrometry; Cousins et al., 2010) should be undertaken to confirm this trend.

As at 25°C, the differences in the temperature dependencies of Rubisco kinetic parameters among C_3 species were not related to the thermal environment of a species' domestication region (data not shown). This finding contrasts with previous evidence suggesting that the temperature sensitivity of Rubisco kinetic properties has evolved to improve the enzyme's performance according to the prevailing thermal environment to which each species is adapted (Sage, 2002; Galmés et al., 2005, 2015).

Although only two C_4 species were included in this study, they presented lower ΔH_a for K_c and for k_{cat}^c than most of the C_3 species, in close agreement with trends observed recently by Perdomo et al. (2015a) in *Flaveria* spp. (Table III). A larger number of C_4 species need to be surveyed to verify the existence of differences in the temperature dependence of Rubisco kinetics between C_3 and C_4 species.

How Do the Species-Specific Properties of Rubisco Kinetics and Their Temperature Sensitivity Impact the Potential Capacity of Rubisco to Assimilate CO_2?

Modeling the effect of the species-specific Rubisco kinetics and temperature dependencies of Rubisco kinetics resulted in significant differences in $A_{Rubisco}$ among the studied C_3 crops (Fig. 2). This modeling exercise highlighted which species would most benefit from the genetic replacement of their native version of Rubisco by other foreign versions with improved performance. Notably, the modeling results clearly indicate that the performance of specific Rubiscos cannot be evaluated without considering the environmental conditions during catalysis, specifically the temperature and the C_c. This fact results from the different temperature dependencies of Rubisco kinetics among crops and from the different impacts that Rubisco kinetics have on the A_c and A_j governing $A_{Rubisco}$. Hence, at 15°C and C_c of 250 μbar, $A_{Rubisco}$ was limited by A_j in most C_3 species (12 out of 18), while it was limited by A_c in all C_3 species at 25°C and 35°C irrespective of the C_c value.

Detailed examination of modeled $A_{Rubisco}$ suggests that future efforts to enhance Rubisco efficiency should be directed at the following C_3 species displaying the poorest performance: *C. maxima* and *M. sativa* at 15°C and both C_c values; *G. max*, *C. annuum*, and *C. arabica* at 25°C and 250 μbar; *G. max*, *S. oleracea*, *C. annuum*, and *C. arabica* at 25°C and 150 μbar; *C. annuum*, *S. lycopersicum*, and *L. sativa* at 35°C and 250 μbar; and *C. annuum* and *S. lycopersicum* at 35°C and 150 μbar.

In order to focus on the Rubisco catalytic traits, the modeling assumed invariable values for E (25 μmol m^{-2} s^{-1}) and specific values for the rate of photosynthetic electron transport (J) and C_c. However, species adapt and plants acclimate to the prevailing thermal environment through changes in the concentration and/or activation of Rubisco and J (Yamasaki et al., 2002; Yamori et al., 2011). Similarly, stomatal and leaf mesophyll conductances to CO_2 also vary in response to temperature (von Caemmerer and Evans, 2015). The growth temperature effects on these parameters would have altered the equilibrium between A_c and A_j and, indirectly, the consequences of different Rubisco kinetic traits on the CO_2 assimilation potential. In the future, we aim to increase the accuracy of the present simulation by examining and including the species-specific values for stomatal and leaf mesophyll conductances, E, and J at varying environmental conditions.

The Analysis of Positive Selection in Branches Leading to Specific Rubisco Traits May Reveal Lineage-Specific Amino Acid Substitutions

We found 10 Rubisco L-subunit residues under positive selection (94, 262, 281, 309, 439, 446, 449, 469, 470, and 477; Table IV). With the exceptions of residues 469 and 477, these residues have been reported previously in other groups of plants, implying a relatively limited number of residues responsible for the Rubisco fine-tuning (Kapralov and Filatov, 2007; Christin et al., 2008; Iida et al., 2009; Kapralov et al., 2011, 2012; Galmés et al., 2014a, 2014c). However, despite widespread parallel evolution of amino acid replacements in the Rubisco sequence, solutions found in particular groups of plants may be quite different. For instance, there are only two common residues under positive selection out of 10 between this study and methodologically similar work with a different sampling design published earlier (Galmés et al., 2014c). This fact raises questions of epistatic interactions and residue coevolution within Rubisco (Wang et al., 2011) as well as residue coevolution and complementarity between Rubisco and its chaperones (Whitney et al., 2015), which both may prevent the evolution of identical amino acid replacements because of different genetic backgrounds.

We have not examined the species differences in the sequence of the Rubisco S-subunit. Some of the species included in this survey, like *T. aestivum*, possess a large number of S-subunit genes (*rbcS*) encoding different

S-subunits (Galili et al., 1998). Previous reports have showed that species with identical L-subunits might have different Rubisco kinetics (Rosnow et al., 2015) and directly demonstrated that differences in the S-subunits might affect Rubisco catalytic traits (Ishikawa et al., 2011; Morita et al., 2014). Therefore, we cannot reject the idea that the observed differences in Rubisco kinetics, and their temperature dependence, among the studied crops are partially due to differences in the S-subunits.

CONCLUSION

This study confirms the significant variation in carboxylation efficiency and parameters that contribute to it among plant species and, to our knowledge, for the first time, provides full Rubisco kinetic profiles for the 20 most important crop species. Our data set could be used as an input for the next generation of species-specific models of leaf photosynthesis and its response to climate change, leading to more precise forecasts of changes in crop productivity and yield. These data could help to decide in which crops the CO_2 assimilation potential and carboxylation efficiency of Rubisco might be improved via reengineering of native enzymes or by replacement with foreign ones, as there is no a one-size-fits-all solution. The design of future attempts at Rubisco engineering in crops should be based on surveys of Rubisco catalytic and genetic diversity with a particular stress on relatives of the crops in question. Growing knowledge of the Rubisco catalytic spectrum combined with existing engineering toolkits for Rubisco (Whitney and Sharwood 2008) and its chaperones (Whitney et al., 2015) give us hope that the Rubisco efficiency, and hence the photosynthetic capacity, of crops could be improved in the near future.

MATERIALS AND METHODS

Species Selection and Growth Conditions

The following 20 crop species were selected for study: *Avena sativa* 'Forridena', *Beta vulgaris* 'Detroit', *Brassica oleracea* var *italica* 'Calabres', *Capsicum annuum* 'Picante', *Coffea arabica* 'Catuaí Vermelho IAC 44', *Cucurbita maxima* 'Totanera', *Glycine max* 'Ransom', *Hordeum vulgare* ssp. *vulgare* 'Morex', *Ipomoea batatas* 'Rosa de Málaga', *Lactuca sativa* 'Cogollo de Tudela', *Manihot esculenta*, *Medicago sativa* 'Aragón', *Oryza sativa* 'Bomba', *Phaseolus vulgaris* 'Contender', *Saccharum* × *officinarum* (hybrid between *Saccharum officinarum* and *Saccharum spontaneum*), *Solanum lycopersicum* 'Roma VF', *Solanum tuberosum* 'Erlanger', *Spinacia oleracea* 'Butterfly', *Triticum aestivum* 'Cajeme', and *Zea mays* 'Carella'. These species represent the most important crops in terms of worldwide production (http://faostat.fao.org/). *C. arabica* was selected as being the most important commodity in the international agricultural trade (DaMatta, 2004). Plants were grown from seeds under natural photoperiods in a glasshouse at the University of the Balearic Islands (Spain) during 2011 and 2012. Plants were grown in soil-based compost supplemented with slow-release fertilizer and frequently watered to avoid water stress. The air temperature in the glasshouse during the growth period was maintained between 15°C and 30°C.

Determination of K_c and k_{cat}^c

Rubisco K_c and K_c^{air} were determined in crude extracts obtained as detailed by Galmés et al. (2014a). Rates of $^{14}CO_2$ fixation were measured at 15°C, 25°C, and 35°C using activated protein extracts in 7-mL septum-capped scintillation vials containing reaction buffer (100 mM Bicine-NaOH, pH 8, 20 mM $MgCl_2$, 0.4 mM RuBP, and about 100 W-A units of carbonic anhydrase) equilibrated previously with either N_2 or a mixture of oxygen and N_2 (21:79). Nine different concentrations of $H^{14}CO_3^-$ (0.1 to 9.4 mM, each with a specific radioactivity of 3.7×10^{10} Bq mol^{-1}) were prepared in the scintillation vials as described previously (Galmés et al., 2014a). Assays at 35°C using Rubisco from C_4 species required increasing $H^{14}CO_3^-$ up to 17.7 mM to reach saturating CO_2 concentration in the aqueous phase. Assays were started by the addition of 10 μL of protein extract and stopped after 1 min by injection of 0.1 mL of 10 M formic acid. Acid-stable ^{14}C was determined by liquid scintillation counting (LS 6500 Multi-Purpose Scintillation Counter; Beckman Coulter) following the removal of acid-labile ^{14}C by evaporation. K_c and K_c^{air} were determined from the fitted data as described elsewhere (Bird et al., 1982). Replicate measurements (n = 3–6) were made using different biological replicates for each species.

To obtain k_{cat}^c, the maximum rate of carboxylation was extrapolated from the Michaelis-Menten fit and divided by the number of Rubisco active sites in solution, quantified by [^{14}C]CABP binding (Yokota and Canvin, 1985). Additional control assays undertaken as detailed by Galmés et al. (2014a) confirmed that the observed acid-stable ^{14}C signal was uniquely the result of Rubisco catalytic activity.

Determination of $S_{c/o}$

Rubisco $S_{c/o}$ was measured on purified extracts obtained as described by Gago et al. (2013). On the day of $S_{c/o}$ measurement, highly concentrated Rubisco solutions were desalted by centrifugation through G-25 Sephadex columns equilibrated previously with CO_2-free 0.1 M Bicine (pH 8.2) containing 20 mM $MgCl_2$. The desalted solutions were made 10 mM with $NaH^{14}CO^3$ (1.85×10^{12} Bq mol^{-1}) and 4 mM NaH_2PO_4 to activate Rubisco by incubation at 37.5°C for 40 min. Reaction mixtures were prepared in oxygen electrodes (Oxygraph; Hansatech Instruments) by first adding 0.95 mL of CO_2-free assay buffer (100 mM Bicine, pH 8.2, 20 mM $MgCl_2$, containing 0.015 mg of carbonic anhydrase). After the addition of 0.02 mL of 0.1 M $NaH^{14}CO_3$ (1.85×10^{12} Bq mol^{-1}), the plug was fitted to the oxygen electrode vessel and enough activated Rubisco (20 μL) was added. The reaction was started by the injection of 10 μL of 25 mM RuBP to be completed between 2 and 7 min depending on the assay temperature. RuBP oxygenation was calculated from the oxygen consumption, and carboxylation was calculated from the amount of ^{14}C incorporated into PGA when all the RuBP had been consumed (Galmés et al., 2014a). Measurements were performed at 15°C, 25°C, and 35°C, with three to nine biological replicates for each species and assayed temperature.

For all Rubisco assays, pH of the assay buffers was accurately adjusted at each temperature of measurement. The concentration of CO_2 in solution in equilibrium with HCO_3^- was calculated assuming a pK_a for carbonic acid of 6.19, 6.11, and 6.06 at 15°C, 25°C, and 35°C, respectively. The concentration of oxygen in solution was assumed to be 305.0, 253.4, and 219.4 nmol mL^{-1} at 15°C, 25°C, and 35°C, respectively (Truesdale and Downing, 1954).

Temperature Dependence Parameters of Rubisco Kinetics

To determine the temperature response of the Rubisco kinetic parameters from each species, values for K_c, K_c^{air}, and $S_{c/o}$ were first converted from concentrations to partial pressures. For this, solubilities for CO_2 were considered to be 0.045, 0.034, and 0.0262 mol L^{-1} bar^{-1} at 15°C, 25°C, and 35°C, respectively. In turn, solubilities for oxygen of 0.0016, 0.0013, and 0.0011 mol L^{-1} bar^{-1} were used at 15°C, 25°C, and 35°C, respectively. The Γ^* was obtained from $S_{c/o}$ as described by von Caemmerer (2000) using the above solubilities for oxygen. Thereafter, values of K_c, Γ^*, and k_{cat}^c at the three temperatures were fitted to an Arrhenius-type equation (Badger and Collatz, 1977; Harley and Tenhunen, 1991):

$$Parameter = \exp\left[c - \frac{\Delta H_a}{RT_k}\right] \quad (1)$$

where c is a scaling constant, R is the molar gas constant (8.314 J K^{-1} mol^{-1}), and T_k is the absolute assay temperature.

CO_2 Assimilation Potential of Crop Rubiscos at Varying Temperatures and CO_2 Availability

According to the biochemical model of C_3 photosynthesis (Farquhar et al., 1980), $A_{Rubisco}$ is defined as the minimum of A_c and A_j:

$$A_{\text{Rubisco}} = \min(A_c, A_j), \quad (2)$$

$$A_c = \frac{k_{cat}^c \cdot E \cdot (C_c - \Gamma^*)}{C_c + K_c^{air}} \quad (3)$$

$$A_j = \frac{(C_c - \Gamma^*) J}{4C_c + 8\Gamma^*} \quad (4)$$

A_{Rubisco} was obtained for each species at three different temperatures (15°C, 25°C, and 35°C) and two different C_c values (150 and 250 μbar), simulating situations of moderate water-stress and well-watered conditions in C_3 plants, respectively (Flexas et al., 2006). The Rubisco catalytic traits k_{cat}^c, Γ^*, and K_c^{air} were taken from the species- and temperature-specific data obtained in this study. E was assumed to be invariable at 25 μmol m^{-2}. Values of J were assumed to be 60, 150, and 212 μmol m^{-2} s^{-1} at 15°C, 25°C, and 35°C, respectively, for all species. At 25°C, J = 150 μmol m^{-2} s^{-1} matches very well with a $J/(k_{cat}^c \times E)$ ratio of 1.5 (Egea et al., 2011). Values for J at 15°C and 35°C were obtained from the J temperature response described for *Nicotiana tabacum* by Walker et al. (2013).

Analysis of Rubisco L-Subunit Sites under Positive Selection

Full-length DNA sequences of the Rubisco L-subunit-encoding gene, *rbcL* (Supplemental Fig. S3), and two additional chloroplast genes (*matK* and *ndhF*) were obtained from GenBank (http://www.ncbi.nlm.nih.gov/genbank/) for the 20 studied species.

DNA sequences were translated into protein sequences for alignment using MUSCLE (Edgar, 2004). The software MODELTEST 3.7 (Posada and Crandall, 1998; Posada and Buckley, 2004) was used to check for the best model before running the phylogenetic analyses. The species phylogeny was reconstructed using concatenated alignment of all three chloroplast genes and maximum-likelihood inference conducted with RAxML version 7.2.6 (Stamatakis, 2006).

Amino acid residues under positive selection were identified using codon-based substitution models in comparative analysis of protein-coding DNA sequences within the phylogenetic framework (Yang, 1997). Given the conservative assumption of no selective pressure at synonymous sites, codon-based substitution models assume that codons with a ratio of nonsynonymous to synonymous substitution rate (d_N/d_S) < 1 evolve under purifying selection to keep protein function and properties, while codons with $d_N/d_S > 1$ evolve under positive Darwinian selection to modify properties of the given protein (Yang, 1997).

The codeml program in the PAML version 4.7 package (Yang, 2007) was used to perform branch site tests of positive selection along prespecified foreground branches (Yang et al., 2005; Yang, 2007). The codeml A model allows $0 \le d_N/d_S \le 1$ and $d_N/d_S = 1$ for all branches. $d_N/d_S > 1$ is permitted only along prespecified foreground branches, and $0 \le d_N/d_S \le 1$ and $d_N/d_S = 1$ is permitted on background branches. Branches leading to species with high or low K_c, k_{cat}^c, $S_{c/o}$, and ΔH_a were marked as foreground branches. For the purpose of these tests, high or low K_c, k_{cat}^c, and $S_{c/o}$ ranges were taken only at 25°C, because of high correlation between values for these kinetic parameters obtained at three different temperatures. ΔH_a for these kinetic parameters also was considered. The A model was used to identify the amino acid sites under positive selection and to calculate the posterior probability of an amino acid belonging to a class with $d_N/d_S > 1$ using the Bayes empirical Bayes approach implemented in PAML (Yang et al., 2005).

The Rubisco L-subunit residues were numbered based on the *S. oleracea* sequence. The location of sites under positive selection was done using the Rubisco protein structure from *S. oleracea* obtained from the RCSB Protein Data Bank (http://www.rcsb.org; file 1RCX; Karkehabadi et al., 2003).

Statistical Analysis

Statistical analysis consisted of one-way ANOVA and correlation for linear regressions. For all the parameters studied, a univariate model of fixed effects was assumed. The univariate general linear model for unbalanced data (Proc. GLM) was applied, and significant differences among species and groups of species were revealed by Duncan tests using IBM SPSS Statistics for Macintosh, version 21.0. The relationships among the kinetic parameters and the temperature dependence parameters were tested with the square of the correlation coefficient observed for linear regressions using the tool implemented in R 3.1.1 (http://www.R-project.org). All statistical tests were considered significant at $P < 0.05$.

The PCC was calculated between pairwise combinations of the kinetic parameters K_c, K_c^{air}, k_{cat}^c, and $S_{c/o}$ at the three temperatures of measurement. However, correlations arising within groups of related taxa might reflect phylogenetic signal rather than true cause-effect relationships, because closely related taxa are not necessarily independent data points and could violate the assumption of randomized sampling employed by conventional statistical methods (Felsenstein, 1985). To overcome this issue, tests were performed for the presence of phylogenetic signal in the data, and trait correlations were calculated with PICs using the AOT module of PHYLOCOM (Webb et al., 2008) using the species phylogeny based on the three chloroplast genes (see below). All these tests were considered significant at $P < 0.05$.

Accession Numbers

Sequence data from this article can be found in the GenBank/EMBL data libraries under accession numbers.

Supplemental Data

The following supplemental materials are available.

Supplemental Figure S1. Box-plot depiction of Rubisco kinetic parameters (K_c, K_c^{air}, k_{cat}^c, and $S_{c/o}$) at 15°C, 25°C, and 35°C when considering the 18 C_3 species alone.

Supplemental Figure S2. Maximum-likelihood phylogeny created using *rbcL*, *matK*, and *ndhF* for the selected crop species.

Supplemental Figure S3. Rubisco L-subunit amino acid alignment for the 20 crop species used in this study.

Supplemental Table S1. Rubisco kinetic parameters measured at 15°C and 35°C for the selected crop species.

ACKNOWLEDGMENTS

We thank Trinidad Garcia for technical help and organization of the radioisotope installation at the Serveis Científico-Tècnics of the Universitat de les Illes Balears (UIB) while running these experiments; Miquel Truyols and collaborators of UIB Experimental Field and Greenhouses; Dr. Arantxa Molins (UIB) for experimental help; Dr. Cyril Douthe, Dr. Josep Cifre, Patricia González, and Dr. Jorge Gago (UIB) for help in improving different parts of the article; and Jaume Jaume and Dr. Sebastià Martorell (UIB) for providing some plant material used in the experiments.

Received April 19, 2016; accepted June 17, 2016; published June 21, 2016.

LITERATURE CITED

Badger MR (1980) Kinetic properties of ribulose 1,5-bisphosphate carboxylase/oxygenase from *Anabaena variabilis*. Arch Biochem Biophys **201:** 247–254

Badger MR, Collatz GJ (1977) Studies on the kinetic mechanism of ribulose-1,5-bisphosphate carboxylase and oxygenase reactions, with particular reference to the effect of temperature on kinetic parameters. Carnegie Inst Wash Year Book **76:** 355–361

Balaguer L, Afif D, Dizengremel P, Dreyer E (1996) Specificity factor of ribulose bisphosphate carboxylase/oxygenase of *Quercus robur*. Plant Physiol Biochem **34:** 879–883

Bermúdez MA, Galmés J, Moreno I, Mullineaux PM, Gotor C, Romero LC (2012) Photosynthetic adaptation to length of day is dependent on S-sulfocysteine synthase activity in the thylakoid lumen. Plant Physiol **160:** 274–288

Bernacchi CJ, Portis AR, Nakano H, von Caemmerer S, Long SP (2002) Temperature response of mesophyll conductance: implications for the determination of Rubisco enzyme kinetics and for limitations to photosynthesis in vivo. Plant Physiol **130:** 1992–1998

Bernacchi CJ, Singsaas EL, Pimentel C, Portis AR Jr, Long SP (2001) Improved temperature response functions for models of Rubisco-limited photosynthesis. Plant Cell Environ **24:** 253–259

Bird IF, Cornelius MJ, Keys AJ (1982) Affinity of RuBP carboxylases for carbon dioxide and inhibition of the enzymes by oxygen. J Exp Bot **33:** 1004–1013

Bota J, Flexas J, Keys AJ, Loveland J, Parry MAJ, Medrano H (2002) CO_2/O_2 specificity factor of ribulose-1,5-bisphosphate carboxylase/oxygenase in grapevines (*Vitis vinifera* L.): first *in vitro* determination and comparison to *in vivo* estimations. Vitis **41:** 163

Bremer B, Bremer K, Chase M, Fay M, Reveal J, Soltis D, Stevens P (2009) An update of the Angiosperm Phylogeny Group classification for the orders and families of flowering plants: APG III. Bot J Linn Soc **161:** 105–121

Brooks A, Farquhar GD (1985) Effect of temperature on the CO_2/O_2 specificity of ribulose-1,5-bisphosphate carboxylase/oxygenase and the rate of respiration in the light: estimates from gas-exchange measurements on spinach. Planta **165:** 397–406

Castrillo M (1995) Ribulose-1,5-bis-phosphate carboxylase activity in altitudinal populations of *Espeletia schultzii* Wedd. Oecologia **101:** 193–196

Chabot BF, Chabot JF, Billings WD (1972) Ribulose-1,5-diphosphate carboxylase activity in arctic and alpine populations of *Oxyria digyna*. Photosynthetica **6:** 364–369

Christin PA, Salamin N, Muasya AM, Roalson EH, Russier F, Besnard G (2008) Evolutionary switch and genetic convergence on *rbcL* following the evolution of C_4 photosynthesis. Mol Biol Evol **25:** 2361–2368

Cousins AB, Ghannoum O, von Caemmerer S, Badger MR (2010) Simultaneous determination of Rubisco carboxylase and oxygenase kinetic parameters in *Triticum aestivum* and *Zea mays* using membrane inlet mass spectrometry. Plant Cell Environ **33:** 444–452

DaMatta FM (2004) Exploring drought tolerance in coffee: a physiological approach with some insights for plant breeding. Braz J Plant Physiol **16:** 1–6

Delgado E, Medrano H, Keys AJ, Parry MAJ (1995) Species variation in Rubisco specificity factor. J Exp Bot **46:** 1775–1777

Díaz-Espejo A (2013) New challenges in modelling photosynthesis: temperature dependencies of Rubisco kinetics. Plant Cell Environ **36:** 2104–2107

Du YC, Peddi SR, Spreitzer RJ (2003) Assessment of structural and functional divergence far from the large subunit active site of ribulose-1,5-bisphosphate carboxylase/oxygenase. J Biol Chem **278:** 49401–49405

Edgar RC (2004) MUSCLE: multiple sequence alignment with high accuracy and high throughput. Nucleic Acids Res **32:** 1792–1797

Egea G, González-Real MM, Baille A, Nortes PA, Díaz-Espejo A (2011) Disentangling the contributions of ontogeny and water stress to photosynthetic limitations in almond trees. Plant Cell Environ **34:** 962–979

Farquhar GD, von Caemmerer S, Berry JA (1980) A biochemical model of photosynthetic CO_2 assimilation in leaves of C_3 species. Planta **149:** 78–90

Felsenstein J (1985) Phylogenies and the comparative method. Am Nat **125:** 1–15

Flexas J, Galmés J, Gallé A, Gulías J, Pou A, Ribas-Carbó M, Tomás M, Medrano H (2010) Improving water use efficiency in grapevines: potential physiological targets for biotechnological improvement. Aust J Grape Wine Res **16:** 106–121

Flexas J, Ribas-Carbó M, Bota J, Galmés J, Henkle M, Martínez-Cañellas S, Medrano H (2006) Decreased Rubisco activity during water stress is not induced by decreased relative water content but related to conditions of low stomatal conductance and chloroplast CO_2 concentration. New Phytol **172:** 73–82

Gago J, Coopman RE, Cabrera HM, Hermida C, Molins A, Conesa MÀ, Galmés J, Ribas-Carbó M, Flexas J (2013) Photosynthesis limitations in three fern species. Physiol Plant **149:** 599–611

Galili S, Avivi Y, Feldman M (1998) Differential expression of three *Rbc*S subfamilies in wheat. Plant Sci **139:** 185–193

Galmés J, Andralojc PJ, Kapralov MV, Flexas J, Keys AJ, Molins A, Parry MAJ, Conesa MÀ (2014a) Environmentally driven evolution of Rubisco and improved photosynthesis and growth within the C_3 genus *Limonium* (Plumbaginaceae). New Phytol **203:** 989–999

Galmés J, Conesa MÀ, Díaz-Espejo A, Mir A, Perdomo JA, Niinemets U, Flexas J (2014b) Rubisco catalytic properties optimized for present and future climatic conditions. Plant Sci **226:** 61–70

Galmés J, Flexas J, Keys AJ, Cifre J, Mitchell RAC, Madgwick PJ, Haslam RP, Medrano H, Parry MAJ (2005) Rubisco specificity factor tends to be larger in plant species from drier habitats and in species with persistent leaves. Plant Cell Environ **28:** 571–579

Galmés J, Kapralov MV, Andralojc PJ, Conesa MÀ, Keys AJ, Parry MAJ, Flexas J (2014c) Expanding knowledge of the Rubisco kinetics variability in plant species: environmental and evolutionary trends. Plant Cell Environ **37:** 1989–2001

Galmés J, Kapralov MV, Copolovici LO, Hermida-Carrera C, Niinemets Ü (2015) Temperature responses of the Rubisco maximum carboxylase activity across domains of life: phylogenetic signals, trade-offs, and importance for carbon gain. Photosynth Res **123:** 183–201

Galmés J, Perdomo JA, Flexas J, Whitney SM (2013) Photosynthetic characterization of Rubisco transplantomic lines reveals alterations on photochemistry and mesophyll conductance. Photosynth Res **115:** 153–166

Galmés J, Ribas-Carbó M, Medrano H, Flexas J (2011) Rubisco activity in Mediterranean species is regulated by the chloroplastic CO_2 concentration under water stress. J Exp Bot **62:** 653–665

Ghannoum O, Evans JR, Chow WS, Andrews TJ, Conroy JP, von Caemmerer S (2005) Faster Rubisco is the key to superior nitrogen-use efficiency in NADP-malic enzyme relative to NAD-malic enzyme C_4 grasses. Plant Physiol **137:** 638–650

Gornall J, Betts R, Burke E, Clark R, Camp J, Willett K, Wiltshire A (2010) Implications of climate change for agricultural productivity in the early twenty-first century. Philos Trans R Soc Lond B Biol Sci **365:** 2973–2989

Hall NP, Keys AJ (1983) Temperature dependence of the enzymic carboxylation and oxygenation of ribulose 1,5-bisphosphate in relation to effects of temperature on photosynthesis. Plant Physiol **72:** 945–948

Harley PC, Tenhunen JD (1991) Modeling the photosynthetic response of C_3 leaves to environmental factors. *In* KJ Boote, RS Loomis, eds, Modeling Crop Photosynthesis: From Biochemistry to Canopy. Crop Science Society of America/American Society of Agronomy, Madison, WI, pp 17–39

Haslam RP, Keys AJ, Andralojc PJ, Madgwick PJ, Inger A, Grimsrud A, Eilertsen HC, Parry MAJ (2005) Specificity of diatom Rubisco. *In* K Omasa, I Nouchi, LJ De Kok, eds, Plant Responses to Air Pollution and Global Change. Springer-Verlag, Tokyo, pp 157–164

Iida S, Miyagi A, Aoki S, Ito M, Kadono Y, Kosuge K (2009) Molecular adaptation of *rbcL* in the heterophyllous aquatic plant Potamogeton. PLoS ONE **4:** e4633

Ishikawa C, Hatanaka T, Misoo S, Fukayama H (2009) Screening of high k_{cat} Rubisco among Poaceae for improvement of photosynthetic CO_2 assimilation in rice. Plant Prod Sci **12:** 345–350

Ishikawa C, Hatanaka T, Misoo S, Miyake C, Fukayama H (2011) Functional incorporation of sorghum small subunit increases the catalytic turnover rate of Rubisco in transgenic rice. Plant Physiol **156:** 1603–1611

Jordan DB, Ogren WL (1983) Species variation in kinetic properties of ribulose 1,5-bisphosphate carboxylase/oxygenase. Arch Biochem Biophys **227:** 425–433

Jordan DB, Ogren WL (1984) The CO_2/O_2 specificity of ribulose 1,5-bisphosphate carboxylase/oxygenase: dependence on ribulosebisphosphate concentration, pH and temperature. Planta **161:** 308–313

Kane HJ, Viil J, Entsch B, Paul K, Morell MK, Andrews TJ (1994) An improved method for measuring the CO_2/O_2 specificity of ribulosebisphosphate carboxylase-oxygenase. Funct Plant Biol **21:** 449–461

Kapralov MV, Filatov DA (2007) Widespread positive selection in the photosynthetic Rubisco enzyme. BMC Evol Biol **7:** 73

Kapralov MV, Kubien DS, Andersson I, Filatov DA (2011) Changes in Rubisco kinetics during the evolution of C_4 photosynthesis in *Flaveria* (Asteraceae) are associated with positive selection on genes encoding the enzyme. Mol Biol Evol **28:** 1491–1503

Kapralov MV, Smith JAC, Filatov DA (2012) Rubisco evolution in C_4 eudicots: an analysis of Amaranthaceae sensu lato. PLoS ONE **7:** e52974

Karkehabadi S, Taylor TC, Andersson I (2003) Calcium supports loop closure but not catalysis in Rubisco. J Mol Biol **334:** 65–73

Keenan T, Sabate S, Gracia C (2010) Soil water stress and coupled photosynthesis-conductance models: bridging the gap between conflicting reports on the relative roles of stomatal, mesophyll conductance and biochemical limitations to photosynthesis. Agric For Meteorol **150:** 443–453

Kent SS, Tomany MJ (1995) The differential of the ribulose 1,5-bisphosphate carboxylase/oxygenase specificity factor among higher plants and the potential for biomass enhancement. Plant Physiol Biochem **33:** 71–80

Kubien DS, Whitney SM, Moore PV, Jesson LK (2008) The biochemistry of Rubisco in *Flaveria*. J Exp Bot **59:** 1767–1777

Laing WA, Ogren WL, Hageman RH (1974) Regulation of soybean net photosynthetic CO_2 fixation by the interaction of CO_2, O_2, and ribulose 1,5-diphosphate carboxylase. Plant Physiol **54:** 678–685

Lehnherr B, Mächler F, Nösberger J (1985) Influence of temperature on the ratio of ribulose bisphosphate carboxylase to oxygenase activities and on the ratio of photosynthesis to photorespiration of leaves. J Exp Bot **36:** 1117–1125

Meyer RS, DuVal AE, Jensen HR (2012) Patterns and processes in crop domestication: an historical review and quantitative analysis of 203 global food crops. New Phytol **196:** 29–48

Monson RK, Stidham MA, Williams GJ, Edwards GE, Uribe EG (1982) Temperature dependence of photosynthesis in *Agropyron smithii* Rydb. I. Factors affecting net CO_2 uptake in intact leaves and contribution from ribulose-1,5-bisphosphate carboxylase measured in vivo and in vitro. Plant Physiol **69:** 921–928

Morita K, Hatanaka T, Misoo S, Fukayama H (2014) Unusual small subunit that is not expressed in photosynthetic cells alters the catalytic properties of Rubisco in rice. Plant Physiol **164:** 69–79

Murchie EH, Pinto M, Horton P (2009) Agriculture and the new challenges for photosynthesis research. New Phytol **181:** 532–552

Niinemets U, Wright IJ, Evans JR (2009) Leaf mesophyll diffusion conductance in 35 Australian sclerophylls covering a broad range of foliage structural and physiological variation. J Exp Bot **60:** 2433–2449

Ort DR, Merchant SS, Alric J, Barkan A, Blankenship RE, Bock R, Croce R, Hanson MR, Hibberd JM, Long SP, et al (2015) Redesigning photosynthesis to sustainably meet global food and bioenergy demand. Proc Natl Acad Sci USA **112:** 8529–8536

Ott CM, Smith BD, Portis AR Jr, Spreitzer RJ (2000) Activase region on chloroplast ribulose-1,5-bisphosphate carboxylase/oxygenase: nonconservative substitution in the large subunit alters species specificity of protein interaction. J Biol Chem **275:** 26241–26244

Parry MA, Andralojc PJ, Scales JC, Salvucci ME, Carmo-Silva AE, Alonso H, Whitney SM (2013) Rubisco activity and regulation as targets for crop improvement. J Exp Bot **64:** 717–730

Parry MA, Hawkesford MJ (2012) An integrated approach to crop genetic improvement. J Integr Plant Biol **54:** 250–259

Parry MAJ, Schmidt CNG, Cornelius MJ, Millard BN, Burton S, Gutteridge S, Dyer TA, Keys AJ (1987) Variations in properties of ribulose-1,5-bisphosphate carboxylase from various species related to differences in amino acid sequences. J Exp Bot **38:** 1260–1271

Perdomo JA, Cavanagh AP, Kubien DS, Galmés J (2015a) Temperature dependence of *in vitro* Rubisco kinetics in species of *Flaveria* with different photosynthetic mechanisms. Photosynth Res **124:** 67–75

Perdomo JA, Conesa MÀ, Medrano H, Ribas-Carbó M, Galmés J (2015b) Effects of long-term individual and combined water and temperature stress on the growth of rice, wheat and maize: relationship with morphological and physiological acclimation. Physiol Plant **155:** 149–165

Pons TL, Flexas J, von Caemmerer S, Evans JR, Genty B, Ribas-Carbó M, Brugnoli E (2009) Estimating mesophyll conductance to CO_2: methodology, potential errors, and recommendations. J Exp Bot **60:** 2217–2234

Posada D, Buckley TR (2004) Model selection and model averaging in phylogenetics: advantages of Akaike information criterion and Bayesian approaches over likelihood ratio tests. Syst Biol **53:** 793–808

Posada D, Crandall KA (1998) MODELTEST: testing the model of DNA substitution. Bioinformatics **14:** 817–818

Prins A, Orr DJ, Andralojc PJ, Reynolds MP, Carmo-Silva E, Parry MAJ (2016) Rubisco catalytic properties of wild and domesticated relatives provide scope for improving wheat photosynthesis. J Exp Bot **67:** 1827–1838

Rinehart CA, Tingey SV, Andersen WR (1983) Variability of reaction kinetics for ribulose-1,5-bisphosphate carboxylase in a barley population. Plant Physiol **72:** 76–79

Rogers A (2014) The use and misuse of $V_{c,max}$ in Earth system models. Photosynth Res **119:** 15–29

Rosnow JJ, Evans MA, Kapralov MV, Cousins AB, Edwards GE, Roalson EH (2015) Kranz and single-cell forms of C_4 plants in the subfamily Suaedoideae show kinetic C_4 convergence for PEPC and Rubisco with divergent amino acid substitutions. J Exp Bot **66:** 7347–7358

Roy H, Andrews TJ (2000) Rubisco: assembly and mechanism. *In* RC Leegood, TD Sharkey, S von Caemmerer, eds, Photosynthesis: Physiology and Metabolism. Kluwer, Dordrecht, The Netherlands, pp 53–83

Sage RF (2002) Variation in the k_{cat} of Rubisco in C_3 and C_4 plants and some implications for photosynthetic performance at high and low temperature. J Exp Bot **53:** 609–620

Sage RF, Cen YP, Li M (2002) The activation state of Rubisco directly limits photosynthesis at low CO_2 and low O_2 partial pressures. Photosynth Res **71:** 241–250

Sage RF, Way DA, Kubien DS (2008) Rubisco, Rubisco activase, and global climate change. J Exp Bot **59:** 1581–1595

Savir Y, Noor E, Milo R, Tlusty T (2010) Cross-species analysis traces adaptation of Rubisco toward optimality in a low-dimensional landscape. Proc Natl Acad Sci USA **107:** 3475–3480

Scafaro AP, Yamori W, Carmo-Silva AE, Salvucci ME, von Caemmerer S, Atwell BJ (2012) Rubisco activity is associated with photosynthetic thermotolerance in a wild rice (*Oryza meridionalis*). Physiol Plant **146:** 99–109

Spreitzer RJ, Salvucci ME (2002) Rubisco: structure, regulatory interactions, and possibilities for a better enzyme. Annu Rev Plant Biol **53:** 449–475

Stamatakis A (2006) RAxML-VI-HPC: maximum likelihood-based phylogenetic analyses with thousands of taxa and mixed models. Bioinformatics **22:** 2688–2690

Tcherkez GG, Farquhar GD, Andrews TJ (2006) Despite slow catalysis and confused substrate specificity, all ribulose bisphosphate carboxylases may be nearly perfectly optimized. Proc Natl Acad Sci USA **103:** 7246–7251

Truesdale GA, Downing AL (1954) Solubility of oxygen in water. Nature **173:** 1236

Uemura K, Anwaruzzaman, Miyachi S, Yokota A (1997) Ribulose-1,5-bisphosphate carboxylase/oxygenase from thermophilic red algae with a strong specificity for CO_2 fixation. Biochem Biophys Res Commun **233:** 568–571

von Caemmerer S (2000) Biochemical Models of Leaf Photosynthesis. CSIRO Publishing, Collingwood, Australia

von Caemmerer S (2013) Steady-state models of photosynthesis. Plant Cell Environ **36:** 1617–1630

von Caemmerer S, Evans JR (2015) Temperature responses of mesophyll conductance differ greatly between species. Plant Cell Environ **38:** 629–637

Walker B, Ariza LS, Kaines S, Badger MR, Cousins AB (2013) Temperature response of *in vivo* Rubisco kinetics and mesophyll conductance in *Arabidopsis thaliana*: comparisons to *Nicotiana tabacum*. Plant Cell Environ **36:** 2108–2119

Wang M, Kapralov MV, Anisimova M (2011) Coevolution of amino acid residues in the key photosynthetic enzyme Rubisco. BMC Evol Biol **11:** 266

Webb CO, Ackerly DD, Kembel SW (2008) Phylocom: software for the analysis of phylogenetic community structure and trait evolution. Bioinformatics **24:** 2098–2100

Weber DJ, Andersen WR, Hess S, Hansen DJ, Gunasekaran M (1977) Ribulose-1,5-bisphosphate carboxylase from plants adapted to extreme environments. Plant Cell Physiol **18:** 693–699

Whitney SM, Birch R, Kelso C, Beck JL, Kapralov MV (2015) Improving recombinant Rubisco biogenesis, plant photosynthesis and growth by coexpressing its ancillary RAF1 chaperone. Proc Natl Acad Sci USA **112:** 3564–3569

Whitney SM, Houtz RL, Alonso H (2011) Advancing our understanding and capacity to engineer nature's CO_2-sequestering enzyme, Rubisco. Plant Physiol **155:** 27–35

Whitney SM, Sharwood RE (2008) Construction of a tobacco master line to improve Rubisco engineering in chloroplasts. J Exp Bot **59:** 1909–1921

Yamasaki T, Yamakawa T, Yamane Y, Koike H, Satoh K, Katoh S (2002) Temperature acclimation of photosynthesis and related changes in photosystem II electron transport in winter wheat. Plant Physiol **128:** 1087–1097

Yamori W, Nagai T, Makino A (2011) The rate-limiting step for CO_2 assimilation at different temperatures is influenced by the leaf nitrogen content in several C_3 crop species. Plant Cell Environ **34:** 764–777

Yamori W, Noguchi K, Hikosaka K, Terashima I (2010) Phenotypic plasticity in photosynthetic temperature acclimation among crop species with different cold tolerances. Plant Physiol **152:** 388–399

Yamori W, Suzuki K, Noguchi K, Nakai M, Terashima I (2006) Effects of Rubisco kinetics and Rubisco activation state on the temperature dependence of the photosynthetic rate in spinach leaves from contrasting growth temperatures. Plant Cell Environ **29:** 1659–1670

Yamori W, von Caemmerer S (2009) Effect of Rubisco activase deficiency on the temperature response of CO_2 assimilation rate and Rubisco

activation state: insights from transgenic tobacco with reduced amounts of Rubisco activase. Plant Physiol **151:** 2073–2082

Yang Z (1997) PAML: a program package for phylogenetic analysis by maximum likelihood. Comput Appl Biosci **13:** 555–556

Yang Z (2007) PAML 4: phylogenetic analysis by maximum likelihood. Mol Biol Evol **24:** 1586–1591

Yang Z, Wong WS, Nielsen R (2005) Bayes empirical Bayes inference of amino acid sites under positive selection. Mol Biol Evol **22:** 1107–1118

Yeoh HH, Badger MR, Watson L (1980) Variations in $K_m(CO_2)$ of ribulose-1,5-bisphosphate carboxylase among grasses. Plant Physiol **66:** 1110–1112

Yeoh HH, Badger MR, Watson L (1981) Variations in kinetic properties of ribulose-1,5-bisphosphate carboxylases among plants. Plant Physiol **67:** 1151–1155

Yokota A, Canvin DT (1985) Ribulose bisphosphate carboxylase/oxygenase content determined with [^{14}C]carboxypentitol bisphosphate in plants and algae. Plant Physiol **77:** 735–739

Zhu XG, Jensen RG, Bohnert HJ, Wildner GF, Schlitter J (1998) Dependence of catalysis and CO_2/O_2 specificity of Rubisco on the carboxy-terminus of the large subunit at different temperatures. Photosynth Res **57:** 71–79

Zhu XG, Long SP, Ort DR (2010) Improving photosynthetic efficiency for greater yield. Annu Rev Plant Biol **61:** 235–261